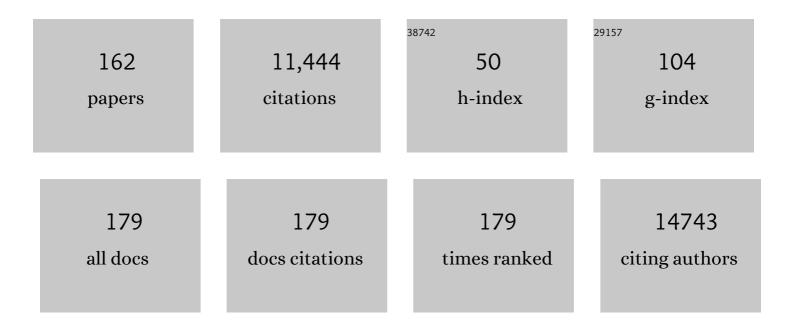
List of Publications by Year in descending order

Source: https://exaly.com/author-pdf/3145000/publications.pdf Version: 2024-02-01



HYUNIOON SONG

#	Article	IF	CITATIONS
1	Bimetallic Gold–Silver Nanostructures Drive Low Overpotentials for Electrochemical Carbon Dioxide Reduction. ACS Applied Materials & Interfaces, 2022, 14, 6604-6614.	8.0	14
2	Nanoparticle design and assembly for p-type metal oxide gas sensors. Nanoscale, 2022, 14, 3387-3397.	5.6	17
3	Inspiration of Yolk-Shell Nanostructures Toward Completely Adjustable Heterogeneous Catalysts. Nanostructure Science and Technology, 2021, , 413-424.	0.1	0
4	Structural complexity induced by {110} blocking of cysteine in electrochemical copper deposition on silver nanocubes. Nanoscale, 2021, 13, 1777-1783.	5.6	8
5	Abnormal Hypsochromic Shifts of Surface Plasmon Scattering by Atomic Ordering in Gold–Copper Intermetallic Nanoparticles. Journal of Physical Chemistry C, 2021, 125, 19936-19946.	3.1	7
6	Surface overgrowth on gold nanoparticles modulating high-energy facets for efficient electrochemical CO2 reduction. Nanoscale, 2021, 13, 14346-14353.	5.6	4
7	Optimal Length of Hybrid Metal–Semiconductor Nanorods for Photocatalytic Hydrogen Generation. ACS Catalysis, 2021, 11, 13303-13311.	11.2	14
8	A highly smart MEMS acetone gas sensors in array for diet-monitoring applications. Micro and Nano Systems Letters, 2021, 9, .	3.7	4
9	Strategies for Designing Nanoparticles for Electro―and Photocatalytic CO <sub>2</sub> Reduction. Chemistry - an Asian Journal, 2020, 15, 253-265.	3.3	9
10	Tracking Underpotential Deposition of Copper on Individual Silver Nanocubes by Real-Time Single-Particle Plasmon Scattering Imaging. Journal of Physical Chemistry C, 2020, 124, 20398-20409.	3.1	18
11	Fe <sub><i>x</i></sub> Ni <sub>2–<i>x</i></sub> P Alloy Nanocatalysts with Electron-Deficient Phosphorus Enhancing the Hydrogen Evolution Reaction in Acidic Media. ACS Catalysis, 2020, 10, 11665-11673.	11.2	41
12	Characterization of heterogeneous aryl–Pd( <scp>ii</scp> )–oxo clusters as active species for C–H arylation. Chemical Communications, 2020, 56, 14404-14407.	4.1	8
13	ZnO–CuO Core-Hollow Cube Nanostructures for Highly Sensitive Acetone Gas Sensors at the ppb Level. ACS Applied Materials & Interfaces, 2020, 12, 35688-35697.	8.0	126
14	In Situ Monitoring of Individual Plasmonic Nanoparticles Resolves Multistep Nanoscale Sulfidation Reactions Hidden by Ensemble Average. Journal of Physical Chemistry C, 2019, 123, 23113-23123.	3.1	5
15	A feasible strategy to prepare quantum dot-incorporated carbon nanofibers as free-standing platforms. Nanoscale Advances, 2019, 1, 3948-3956.	4.6	1
16	Artificial Control of Cell Signaling Using a Photocleavable Cobalt(III)–Nitrosyl Complex. Angewandte Chemie, 2019, 131, 10232-10237.	2.0	4
17	Surface activation of cobalt oxide nanoparticles for photocatalytic carbon dioxide reduction to methane. Journal of Materials Chemistry A, 2019, 7, 15068-15072.	10.3	33
18	Artificial Control of Cell Signaling Using a Photocleavable Cobalt(III)–Nitrosyl Complex. Angewandte Chemie - International Edition, 2019, 58, 10126-10131.	13.8	15

#	Article	IF	CITATIONS
19	Branched Copper Oxide Nanoparticles Induce Highly Selective Ethylene Production by Electrochemical Carbon Dioxide Reduction. Journal of the American Chemical Society, 2019, 141, 6986-6994.	13.7	260
20	Regulation of electron-hole recombination kinetics on uniform metal-semiconductor nanostructures for photocatalytic hydrogen evolution. APL Materials, 2019, 7, 100702.	5.1	11
21	Nano-Protrusive Gold Nanoparticle-Hybridized Polymer Thin Film as a Sensitive, Multipatternable, and Antifouling Biosensor Platform. ACS Applied Materials & Interfaces, 2018, 10, 13397-13405.	8.0	12
22	Single-Molecule Rotation for EGFR Conformational Dynamics in Live Cells. Journal of the American Chemical Society, 2018, 140, 15161-15165.	13.7	24
23	Metal–CdSe Double Shell Hollow Nanocubes via Sequential Nanoscale Reactions and Their Photocatalytic Hydrogen Evolution. Topics in Catalysis, 2018, 61, 965-976.	2.8	1
24	Composition effect of alloy semiconductors on Pt-tipped Zn <sub>1â^'x</sub> Cd <sub>x</sub> Se nanorods for enhanced photocatalytic hydrogen generation. Journal of Materials Chemistry A, 2018, 6, 16316-16321.	10.3	14
25	Effective Formation of WO <sub>3</sub> Nanoparticle/Bi <sub>2</sub> S <sub>3</sub> Nanowire Composite for Improved Photoelectrochemical Performance. Journal of Physical Chemistry C, 2018, 122, 17676-17685.	3.1	19
26	Synthesis of Co/SiO2 hybrid nanocatalyst via twisted Co3Si2O5(OH)4 nanosheets for high-temperature Fischer–Tropsch reaction. Nano Research, 2017, 10, 1044-1055.	10.4	21
27	Preparation and phase transition of FeOOH nanorods: strain effects on catalytic water oxidation. Nanoscale, 2017, 9, 4751-4758.	5.6	50
28	Preparation and Electrochemical Characterization of Carbonaceous Thin Layer. Electroanalysis, 2017, 29, 1062-1068.	2.9	1
29	Directed Câ^'H Activation and Tandem Cross oupling Reactions Using Palladium Nanocatalysts with Controlled Oxidation. Angewandte Chemie, 2017, 129, 7056-7060.	2.0	5
30	Directed Câ^'H Activation and Tandem Cross oupling Reactions Using Palladium Nanocatalysts with Controlled Oxidation. Angewandte Chemie - International Edition, 2017, 56, 6952-6956.	13.8	35
31	Rh(0)/Rh( <scp>iii</scp> ) core–shell nanoparticles as heterogeneous catalysts for cyclic carbonate synthesis. Chemical Communications, 2017, 53, 384-387.	4.1	9
32	Non-native transition metal monoxide nanostructures: unique physicochemical properties and phase transformations of CoO, MnO and ZnO. NPG Asia Materials, 2017, 9, e364-e364.	7.9	28
33	Synthesis of Gold Nanoparticles in Liquid Phase. , 2017, , 165-200.		0
34	Engineering Reaction Kinetics by Tailoring the Metal Tips of Metal–Semiconductor Nanodumbbells. Nano Letters, 2017, 17, 5688-5694.	9.1	31
35	Colloidal zinc oxide-copper(I) oxide nanocatalysts for selective aqueous photocatalytic carbon dioxide conversion into methane. Nature Communications, 2017, 8, 1156.	12.8	126
36	Enhanced Visible Light Activity of Single-Crystalline WO <sub>3</sub> Microplates for Photoelectrochemical Water Oxidation. Journal of Physical Chemistry C, 2016, 120, 9192-9199.	3.1	37

#	Article	IF	CITATIONS
37	Metal–semiconductor double shell hollow nanocubes for highly stable hydrogen generation photocatalysts. Journal of Materials Chemistry A, 2016, 4, 13414-13418.	10.3	30
38	Far-Field and Near-Field Investigation of Longitudinal Plasmons of AgAuAg Nanorods. Journal of Physical Chemistry C, 2016, 120, 21082-21090.	3.1	6
39	Air-stable CuInSe <sub>2</sub> nanoparticles formed through partial cation exchange in methanol at room temperature. CrystEngComm, 2016, 18, 6069-6075.	2.6	11
40	Nonstoichiometric Co-rich ZnCo <sub>2</sub> O <sub>4</sub> Hollow Nanospheres for High Performance Formaldehyde Detection at ppb Levels. ACS Applied Materials & Interfaces, 2016, 8, 3233-3240.	8.0	83
41	Selective formation of Ag domains on MnO nanooctapods for potential dual imaging probes. CrystEngComm, 2016, 18, 4188-4195.	2.6	2
42	A Resonanceâ€Shifting Hybrid nâ€Type Layer for Boosting Nearâ€Infrared Response in Highly Efficient Colloidal Quantum Dots Solar Cells. Advanced Materials, 2015, 27, 8102-8108.	21.0	28
43	Selective Growth and Structural Analysis of Regular MnO Nanooctapods Bearing Multiple Highâ€Index Surface Facets. Chemistry - an Asian Journal, 2015, 10, 1784-1790.	3.3	3
44	Formation of Metal Selenide and Metal–Selenium Nanoparticles using Distinct Reactivity between Selenium and Noble Metals. Chemistry - an Asian Journal, 2015, 10, 1452-1456.	3.3	16
45	Ultrasensitive formaldehyde gas sensors based on a hollow assembly and its 3-dimensional network formation of single-crystalline Co3O4 nanoparticles. , 2015, , .		2
46	Probing the nanoscale Schottky barrier of metal/semiconductor interfaces of Pt/CdSe/Pt nanodumbbells by conductive-probe atomic force microscopy. Nanoscale, 2015, 7, 12297-12301.	5.6	28
47	Metal Hybrid Nanoparticles for Catalytic Organic and Photochemical Transformations. Accounts of Chemical Research, 2015, 48, 491-499.	15.6	83
48	<i>Ex Situ</i> and <i>in Situ</i> Surface Plasmon Monitoring of Temperature-Dependent Structural Evolution in Galvanic Replacement Reactions at a Single-Particle Level. Journal of Physical Chemistry C, 2015, 119, 20125-20135.	3.1	17
49	Surfactant-free Pd@pSiO2 yolk–shell nanocatalysts for selective oxidation of primary alcohols to aldehydes. New Journal of Chemistry, 2015, 39, 8153-8157.	2.8	10
50	Suzuki Coupling Reaction Using Hybrid Pd Nanoparticles. Journal of Nanoscience and Nanotechnology, 2014, 14, 1872-1883.	0.9	6
51	Facile Synthesis of Multipodal MnO Nanocrystals and Their Catalytic Performance. European Journal of Inorganic Chemistry, 2014, 2014, 1279-1283.	2.0	11
52	A highly Lewis-acidic Pd( <scp>iv</scp> ) surface on Pd@SiO <sub>2</sub> nanocatalysts for hydroalkoxylation reactions. Chemical Communications, 2014, 50, 14938-14941.	4.1	33
53	A Hollow Assembly and Its Three-Dimensional Network Formation of Single-Crystalline Co <sub>3</sub> O <sub>4</sub> Nanoparticles for Ultrasensitive Formaldehyde Gas Sensors. Journal of Physical Chemistry C, 2014, 118, 25994-26002.	3.1	62
54	Anti-counterfeit nanoscale fingerprints based on randomly distributed nanowires. Nanotechnology, 2014, 25, 155303.	2.6	77

#	Article	IF	CITATIONS
55	A chelating effect in hybrid inks for non-vacuum-processed CulnSe2 thin films. Journal of Materials Chemistry A, 2014, 2, 5087.	10.3	23
56	Precise adjustment of structural anisotropy and crystallinity on metal–Fe3O4 hybrid nanoparticles and its influence on magnetic and catalytic properties. Journal of Materials Chemistry C, 2014, 2, 4997-5004.	5.5	18
57	Ultra-low overpotential and high rate capability in Li–O2 batteries through surface atom arrangement of PdCu nanocatalysts. Energy and Environmental Science, 2014, 7, 1362.	30.8	193
58	Au@Ag Core–Shell Nanocubes for Efficient Plasmonic Light Scattering Effect in Low Bandgap Organic Solar Cells. ACS Nano, 2014, 8, 3302-3312.	14.6	228
59	Bovine Serum Albumin as an Effective Surface Regulating Biopolymer for Morphology Control of Gold Polyhedrons. Crystal Growth and Design, 2013, 13, 4131-4137.	3.0	11
60	The growth of Cu2â^'Se thin films using nanoparticles. Thin Solid Films, 2013, 546, 299-307.	1.8	31
61	Poly(ethylene glycol)- and Carboxylate-Functionalized Gold Nanoparticles Using Polymer Linkages: Single-Step Synthesis, High Stability, and Plasmonic Detection of Proteins. Langmuir, 2013, 29, 13518-13526.	3.5	24
62	CuO hollow nanosphere-catalyzed cross-coupling of aryl iodides with thiols. Nanoscale Research Letters, 2013, 8, 390.	5.7	14
63	Terahertz time-domain measurement of non-Drude conductivity in silver nanowire thin films for transparent electrode applications. Applied Physics Letters, 2013, 102, 011109.	3.3	29
64	Carbon layer reduction via a hybrid ink of binary nanoparticles in non-vacuum-processed CuInSe2 thin films. Solar Energy Materials and Solar Cells, 2013, 110, 126-132.	6.2	19
65	Hot Carrier-Driven Catalytic Reactions on Pt–CdSe–Pt Nanodumbbells and Pt/GaN under Light Irradiation. Nano Letters, 2013, 13, 1352-1358.	9.1	101
66	Localized plasmon resonances of bimetallic AgAuAg nanorods. Physical Chemistry Chemical Physics, 2013, 15, 4190-4194.	2.8	11
67	Non-vacuum processed CulnSe2 thin films fabricated with a hybrid ink. Solar Energy Materials and Solar Cells, 2013, 109, 17-25.	6.2	48
68	Azide-Alkyne Huisgen [3+2] Cycloaddition Using CuO Nanoparticles. Molecules, 2012, 17, 13235-13252.	3.8	51
69	Geometric Effect of Single or Double Metal-Tipped CdSe Nanorods on Photocatalytic H <sub>2</sub> Generation. Journal of Physical Chemistry Letters, 2012, 3, 3781-3785.	4.6	83
70	ZnO–CuO core–branch nanocatalysts for ultrasound-assisted azide–alkyne cycloaddition reactions. Chemical Communications, 2012, 48, 8484.	4.1	48
71	Plasmonic Monitoring of Catalytic Hydrogen Generation by a Single Nanoparticle Probe. Journal of the American Chemical Society, 2012, 134, 1221-1227.	13.7	75
72	High-Pressure Adsorption of Ethylene on Cubic Pt Nanoparticles and Pt(100) Single Crystals Probed by in Situ Sum Frequency Generation Vibrational Spectroscopy. ACS Catalysis, 2012, 2, 2377-2386.	11.2	20

#	Article	IF	CITATIONS
73	A hybrid ink of binary copper sulfide nanoparticles and indium precursor solution for a dense CuInSe2 absorber thin film and its photovoltaic performance. Journal of Materials Chemistry, 2012, 22, 17893.	6.7	47
74	New Crystal Structure: Synthesis and Characterization of Hexagonal Wurtzite MnO. Journal of the American Chemical Society, 2012, 134, 8392-8395.	13.7	42
75	Full-Color Tuning of Surface Plasmon Resonance by Compositional Variation of Au@Ag Core–Shell Nanocubes with Sulfides. Langmuir, 2012, 28, 9003-9009.	3.5	71
76	Porosity Control of Pd@SiO <sub>2</sub> Yolk–Shell Nanocatalysts by the Formation of Nickel Phyllosilicate and Its Influence on Suzuki Coupling Reactions. Langmuir, 2012, 28, 6441-6447.	3.5	71
77	Synthesis of Pd/SiO2 Nanobeads for Use in Suzuki Coupling Reactions by Reverse Micelle Sol–gel Process. Catalysis Letters, 2012, 142, 588-593.	2.6	22
78	Shape Evolution and Gram-Scale Synthesis of Gold@Silver Core–Shell Nanopolyhedrons. Journal of Physical Chemistry C, 2011, 115, 9417-9423.	3.1	49
79	Assembly of individual TiO <sub>2</sub> –C <sub>60</sub> <i>/</i> porphyrin hybrid nanoparticles for enhancement of photoconversion efficiency. Nanotechnology, 2011, 22, 275720.	2.6	6
80	Extremely Active Pd@pSiO <sub>2</sub> Yolk–Shell Nanocatalysts for Suzuki Coupling Reactions of Aryl Halides. Journal of Physical Chemistry C, 2011, 115, 15772-15777.	3.1	85
81	The Role of Water for the Phaseâ€Selective Preparation of Hexagonal and Cubic Cobalt Oxide Nanoparticles. Chemistry - an Asian Journal, 2011, 6, 1575-1581.	3.3	10
82	Gram‣cale Synthesis of Magnetically Separable and Recyclable Co@SiO <sub>2</sub> Yolk‣hell Nanocatalysts for Phenoxycarbonylation Reactions. ChemCatChem, 2011, 3, 755-760.	3.7	34
83	Metal@Silica yolk-shell nanostructures as versatile bifunctional nanocatalysts. Nano Research, 2011, 4, 33-49.	10.4	173
84	Coordination Power Adjustment of Surfaceâ€Regulating Polymers for Shaping Gold Polyhedral Nanocrystals. Chemistry - A European Journal, 2011, 17, 8466-8471.	3.3	15
85	Simple fabrication of patterned gold nanoparticle arrays on functionalized block copolymer thin films. European Polymer Journal, 2011, 47, 305-310.	5.4	4
86	Formation of single-domain homogeneous Au nanoparticle monolayer at the water/oil interface and its application to surface-enhanced Raman scattering. Journal of Vacuum Science and Technology B:Nanotechnology and Microelectronics, 2011, 29, 021801.	1.2	1
87	New Synthesis Approach for Low Temperature Bimetallic Nanoparticles: Size and Composition Controlled Sn–Cu Nanoparticles. Journal of Nanoscience and Nanotechnology, 2011, 11, 1037-1041.	0.9	16
88	Solvent-Free Microwave Promoted [3Â+Â2] Cycloaddition of Alkyne-Azide in Uniform CuO Hollow Nanospheres. Topics in Catalysis, 2010, 53, 523-528.	2.8	21
89	Electrochemical deposition of Pd nanoparticles on indium-tin oxide electrodes and their catalytic properties for formic acid oxidation. Electrochemistry Communications, 2010, 12, 1442-1445.	4.7	34
90	Silver/Gold Heterometallic Nanostructures and Their Surface Plasmon-related Behaviors. Materials Research Society Symposia Proceedings, 2010, 1257, 1.	0.1	0

#	Article	IF	CITATIONS
91	Immobilized CuO Hollow Nanospheres Catalyzed Alkyne-Azide Cycloadditions. Journal of Nanoscience and Nanotechnology, 2010, 10, 6504-6509.	0.9	13
92	Platinum-Centered Yolkâ ´`Shell Nanostructure Formation by Sacrificial Nickel Spacers. Langmuir, 2010, 26, 16469-16473.	3.5	29
93	Catalytic Hydrogen Transfer of Ketones over Ni@SiO <sub>2</sub> Yolkâ^'Shell Nanocatalysts with Tiny Metal Cores. Journal of Physical Chemistry C, 2010, 114, 6381-6388.	3.1	77
94	Agâ''Auâ''Ag Heterometal Nanowires: Synthesis, Diameter Control, and Dual Transversal Modes with Diameter Dependency. Journal of Physical Chemistry C, 2010, 114, 12529-12534.	3.1	15
95	Syntheses and Characterization of Wurtzite CoO, Rocksalt CoO, and Spinel Co <sub>3</sub> O <sub>4</sub> Nanocrystals: Their Interconversion and Tuning of Phase and Morphology. Chemistry of Materials, 2010, 22, 4446-4454.	6.7	149
96	CuO hollow nanostructures catalyze [3 + 2] cycloaddition of azides with terminal alkynes. Chemical Communications, 2010, 46, 439-441.	4.1	117
97	Ni@SiO <sub>2</sub> yolk-shell nanoreactor catalysts: High temperature stability and recyclability. Journal of Materials Chemistry, 2010, 20, 1239-1246.	6.7	210
98	Cu2O Nanocubes Catalyzed Difunctionalization Reaction of Vinyl Arenes with Cyclic Ethers. Bulletin of the Korean Chemical Society, 2010, 31, 3509-3510.	1.9	14
99	Monodisperse Pt and PtRu/C60 hybrid nanoparticles for fuel cell anode catalysts. Chemical Communications, 2009, , 5036.	4.1	48
100	Hybrid Gold Architectures for Sensing and Catalytic Applications. Materials Research Society Symposia Proceedings, 2009, 1176, 26.	0.1	0
101	Gramâ€5cale Synthesis of Cu <sub>2</sub> 0 Nanocubes and Subsequent Oxidation to CuO Hollow Nanostructures for Lithiumâ€ion Battery Anode Materials. Advanced Materials, 2009, 21, 803-807.	21.0	613
102	Cu <sub>2</sub> O Nanocubeâ€Catalyzed Crossâ€Coupling of Aryl Halides with Phenols via Ullmann Coupling. European Journal of Inorganic Chemistry, 2009, 2009, 4219-4223.	2.0	65
103	A Selective Fluoroionophore Based on BODIPYâ€functionalized Magnetic Silica Nanoparticles: Removal of Pb <sup>2+</sup> from Human Blood. Angewandte Chemie - International Edition, 2009, 48, 1239-1243.	13.8	178
104	One-Dimensional Gold Nanostructures through Directed Anisotropic Overgrowth from Gold Decahedrons. Journal of Physical Chemistry C, 2009, 113, 3449-3454.	3.1	53
105	A Facile One-Pot Synthesis of Hydroxyl-Functionalized Gold Polyhedrons by a Surface Regulating Copolymer. Chemistry of Materials, 2009, 21, 939-944.	6.7	19
106	Chemical transformation and morphology change of nickel–silica hybrid nanostructures via nickel phyllosilicates. Chemical Communications, 2009, , 7345.	4.1	61
107	Asymmetric Hollow Nanorod Formation through a Partial Galvanic Replacement Reaction. Journal of the American Chemical Society, 2009, 131, 18210-18211.	13.7	97
108	Highly Efficient and Reusable Copper-Catalyzed N-Arylation of Nitrogen-Containing Heterocycles with Aryl Halides. Molecules, 2009, 14, 5169-5178.	3.8	50

#	Article	IF	CITATIONS
109	Shape auxiliary approach for carboxylate-functionalized gold nanocrystals. Chemical Communications, 2009, , 1276.	4.1	4
110	Influence of Particle Size on Reaction Selectivity in Cyclohexene Hydrogenation and Dehydrogenation over Silica-Supported Monodisperse Pt Particles. Catalysis Letters, 2008, 126, 10-19.	2.6	76
111	Directed Surface Overgrowth and Morphology Control of Polyhedral Gold Nanocrystals. Angewandte Chemie - International Edition, 2008, 47, 763-767.	13.8	101
112	Singleâ€Crystalline Hollow Faceâ€Centeredâ€Cubic Cobalt Nanoparticles from Solid Faceâ€Centeredâ€Cubic Cobalt Oxide Nanoparticles. Angewandte Chemie - International Edition, 2008, 47, 9504-9508.	13.8	127
113	A Nanoreactor Framework of a Au@SiO <sub>2</sub> Yolk/Shell Structure for Catalytic Reduction of <i>p</i> â€Nitrophenol. Advanced Materials, 2008, 20, 1523-1528.	21.0	868
114	Kinetics and mechanism of ethylene hydrogenation poisoned by CO on silica-supported monodisperse Pt nanoparticles. Journal of Catalysis, 2008, 254, 1-11.	6.2	52
115	Adsorption and Co-adsorption of Ethylene and Carbon Monoxide on Silica-Supported Monodisperse Pt Nanoparticles:  Volumetric Adsorption and Infrared Spectroscopy Studies. Langmuir, 2008, 24, 198-207.	3.5	64
116	Agâ ''Auâ ''Ag Heterometallic Nanorods Formed through Directed Anisotropic Growth. Journal of the American Chemical Society, 2008, 130, 2940-2941.	13.7	191
117	Shape Adjustment between Multiply Twinned and Single-Crystalline Polyhedral Gold Nanocrystals: Decahedra, Icosahedra, and Truncated Tetrahedra. Journal of Physical Chemistry C, 2008, 112, 2469-2475.	3.1	232
118	Precise Tuning of Porosity and Surface Functionality in Au@SiO <sub>2</sub> Nanoreactors for High Catalytic Efficiency. Chemistry of Materials, 2008, 20, 5839-5844.	6.7	174
119	Platinum Nanoclusters' Size and Surface Structure Sensitivity of Catalytic Reactions. , 2008, , 149-166.		10
120	Synthesis of Polycrystalline Mo/MoOxNanoflakes and Their Transformation to MoO3and MoS2Nanoparticles. Chemistry of Materials, 2007, 19, 2706-2708.	6.7	28
121	1D and 3D Ionic Liquid–Aluminum Hydroxide Hybrids Prepared via an Ionothermal Process. Advanced Functional Materials, 2007, 17, 2411-2418.	14.9	33
122	Surface status and size influences of nickel nanoparticles on sulfur compound adsorption. Applied Surface Science, 2007, 253, 5864-5867.	6.1	49
123	Monodisperse PtRu Nanoalloy on Carbon as a High-Performance DMFC Catalyst. Chemistry of Materials, 2006, 18, 4209-4211.	6.7	74
124	Hydrothermal Growth of Mesoporous SBA-15 Silica in the Presence of PVP-Stabilized Pt Nanoparticles: Synthesis, Characterization, and Catalytic Properties. Journal of the American Chemical Society, 2006, 128, 3027-3037.	13.7	493
125	Polyhedral Gold Nanocrystals withOhSymmetry:Â From Octahedra to Cubes. Journal of the American Chemical Society, 2006, 128, 14863-14870.	13.7	398
126	Monodisperse platinum nanoparticles of well-defined shape: synthesis, characterization, catalytic properties and future prospects. Topics in Catalysis, 2006, 39, 167-174.	2.8	224

#	Article	IF	CITATIONS
127	The synthesis and characterization of Re3(μ-H)3(CO)9â^'n(PMe3)n(μ3-η2:η2:η2-C60) (n=2,3) complexes. Journ of Organometallic Chemistry, 2005, 690, 4704-4711.	al 1.8	11
128	Platinum nanoparticle encapsulation during hydrothermal growth of mesoporous oxides: Synthesis, characterization and catalytic properties. Materials Research Society Symposia Proceedings, 2005, 900, 1.	0.1	0
129	Thermal Wetting of Platinum Nanocrystals on Silica Surface. Journal of Physical Chemistry B, 2005, 109, 6940-6943.	2.6	75
130	High-Surface-Area Catalyst Design:Â Synthesis, Characterization, and Reaction Studies of Platinum Nanoparticles in Mesoporous SBA-15 Silicaâ€. Journal of Physical Chemistry B, 2005, 109, 2192-2202.	2.6	544
131	Pt Nanocrystals:Â Shape Control and Langmuirâ^'Blodgett Monolayer Formation. Journal of Physical Chemistry B, 2005, 109, 188-193.	2.6	510
132	Unusually High Performance Photovoltaic Cell Based on a [60]Fullerene Metal Clusterâ^'Porphyrin Dyad SAM on an ITO Electrode. Journal of the American Chemical Society, 2005, 127, 2380-2381.	13.7	111
133	Structure Sensitivity of Vibrational Spectra of Mesoporous Silica SBA-15 and Pt/SBA-15. Journal of Physical Chemistry B, 2005, 109, 17386-17390.	2.6	71
134	Platonic Gold Nanocrystals. Angewandte Chemie - International Edition, 2004, 43, 3673-3677.	13.8	879
135	Cover Picture: Platonic Gold Nanocrystals (Angew. Chem. Int. Ed. 28/2004). Angewandte Chemie - International Edition, 2004, 43, 3615-3615.	13.8	3
136	Cluster and Polynuclear Compounds. Inorganic Syntheses, 2004, , 184-232.	0.3	3
137	Strong Interfullerene Electronic Communication in a Bisfullereneâ^'Hexarhodium Sandwich Complex. Journal of the American Chemical Society, 2004, 126, 9837-9844.	13.7	28
138	[60]Fullerene—Metal Cluster Complexes: Novel Bonding Modes and Electronic Communication. ChemInform, 2003, 34, no.	0.0	0
139	[60]Fullereneâ^'Metal Cluster Complexes:  Novel Bonding Modes and Electronic Communication. Accounts of Chemical Research, 2003, 36, 78-86.	15.6	160
140	Ligand-Induced Conversion ofï€toïƒC60â^'Metal Cluster Complexes: Full Characterization of theî¼3-î·1:î·2:î·1-C60Bonding Mode. Organometallics, 2002, 21, 2514-2520.	2.3	22
141	Substitution Reactions of aî¼3-î·1:î·2:î·1-C60Triosmium Cluster Complex and Formation of a Novelî¼3-î·1:î·1:î·2-C60Bonding Mode. Organometallics, 2002, 21, 5221-5228.	2.3	9
142	[60]Fullerene as a Versatile Four-Electron Donor Ligand. Organometallics, 2002, 21, 1756-1758.	2.3	21
143	The first observation of four-electron reduction in [60]fullerene-metal cluster self-assembled monolayers (SAMs)Electronic supplementary information (ESI) available: CV spectra, half-wave potentials and XPS data. See http://www.rsc.org/suppdata/cc/b2/b209024d/. Chemical Communications, 2002 2966-2967.	4.1	15
144	The First Fullereneâ^'Metal Sandwich Complex:Â An Unusually Strong Electronic Communication between Two C60Cages. Journal of the American Chemical Society, 2002, 124, 2872-2873.	13.7	71

#	Article	IF	CITATIONS
145	Reversible Interconversion between μ,η2:η2- and μ3,η2:η2:η2-C60on a Carbido Pentaosmium Cluster Framewo Organometallics, 2001, 20, 5564-5570.	rk <sub>2.3</sub>	30
146	Synthesis and Characterization of μ3-η2,η2,η2-C60Trirhenium Hydrido Cluster Complexes. Organometallics, 2001, 20, 3139-3144.	2.3	32
147	First Example of theμ3-η1,η2,η1-C60 Bonding Mode: Ligand-Induced Conversion of π to σ C60-Metal Complexe Angewandte Chemie - International Edition, 2001, 40, 1500-1502.	<sup>'S.</sup> 13.8	33
148	First Example of the Âμ(3)-eta(1),eta(2),eta(1)-C(60) Bonding Mode: Ligand-Induced Conversion of pi to sigma C(60)-Metal Complexes We are grateful to the National Research Laboratory (NRL) Program of Korean Ministry of Science & Technology (MOST) and the Korea Science Engineering Foundation (Project No. 1999-1-122-001-5) for financial support of this research Angewandte Chemie - International Edition, 2001, 40, 1500-1502.	13.8	0
149	C60Self-Assembled Monolayer Using Diamine as a Prelayer. Chemistry Letters, 2000, 29, 958-959.	1.3	8
150	Interconversion between -2,2-C60 and 3-2,2,2-C60 on a Carbido Pentaosmium Cluster Framework. Angewandte Chemie - International Edition, 2000, 39, 1801-1804.	13.8	26
151	Fluxional processes and structural characterization of μ3-η2,η2,η2-C60 triosmium cluster complexes, Os3(CO)9â^'n(PMe3)n(μ3-η2,η2,η2-C60) (n=1, 2, 3). Journal of Organometallic Chemistry, 2000, 599, 49-56.	1.8	25
152	Hydrocarbyl Ligand Transformation on the Tungsten–Triosmium Cluster Framework. Journal of Cluster Science, 2000, 11, 343-358.	3.3	4
153	Synthesis and characterization of (CH3C(CH2PPh2)3)RhH(η2-C60). Journal of Organometallic Chemistry, 1999, 584, 361-365.	1.8	6
154	Synthesis, Structure, and Electrochemical Studies of μ3-η2,η2,η2-C60Triosmium Complexes. Organometallics, 1998, 17, 4477-4483.	2.3	44
155	Reaction of CpWOs3(CO)11(μ3-CTol) with H2S: μ-alkylidene and μ3-alkylidyne WOs3 cluster complexes containing a sulfido ligand. Journal of Organometallic Chemistry, 1998, 558, 71-80.	1.8	6
156	Synthesis, structure, and catalytic properties of ansa-zirconocenes, Me2Si(RInd)2ZrCl2 (R=2-p- or) Tj ETQq0 0 0 r	gBT/Over 1.8	loçk 10 Tf 50
157	Synthesis and Characterization of η2-C60 and μ3-η2,η2,η2-C60 Triosmium Cluster Complexes. Organometallics, 1998, 17, 227-236.	2.3	66
158	Electrochemical Studies of C60â^'Triosmium Complexes:Â First Evidence for a C60-Mediated Electron Transfer to the Metal Center. Inorganic Chemistry, 1997, 36, 2698-2699.	4.0	23
159	Synthesis, structure, and catalytic properties of ansa-Zirconocenes, Me2X(Cp)(RInd) ZrCl2 (X = C, Si; R) Tj ETQq1	1.0,7843 1.8	14 rgBT /Ove
160	Synthesis and characterization of [Me2M-μ-N(H)NMe2]2 (M = Al, Ga). Crystal structure of trans [Me2Al-μ-N(H)NMe2]2. Journal of Organometallic Chemistry, 1997, 545-546, 99-103.	1.8	33
161	Characterization and structures of intermediates in the reactivity of CpWOs3(CO)11(μ3-CTol) towards dihydrogen and water. Journal of Organometallic Chemistry, 1996, 526, 215-225.	1.8	9
162	Triosmium cluster derivatives of [60]fullerene. Journal of the Chemical Society Chemical Communications, 1995, , 15.	2.0	32